

# Wavelength Demultiplexer Using the Spatial Dispersion of Multilayer Thin-Film Structures

Martina Gerken, *Student Member, IEEE*, and David A. B. Miller, *Fellow, IEEE*

**Abstract**—We demonstrate that a single 66-layer nonperiodic thin-film stack can be used to separate four wavelength channels by spatial beam shifting. This device uses group velocity effects similar to the superprism effect observed in photonic crystals, but shows larger and more controlled shifts including constant dispersion allowing for equidistant channel spacing. Experimentally, a nearly linear 100- $\mu\text{m}$  shift is achieved between 827 and 841 nm. System considerations are discussed.

**Index Terms**—Dispersive media, nanotechnology, nonhomogeneous media, wavelength-division multiplexing.

WAVELENGTH-DIVISION-MULTIPLEXING (WDM) systems create a strong need for compact, cost-effective wavelength multiplexing and demultiplexing devices. We focus here on thin-film structures, since they are easy to fabricate with well-known technology. In contrast to typical dielectric interference filters though, we use group velocity effects to separate multiple beams of different wavelengths with a single multilayer structure. These group velocity effects are similar to the superprism effect observed in one-dimensional [1], [2], two-dimensional [1], [3], [4], and three-dimensional [5] photonic crystals. The multilayer thin-film stack is designed such that different wavelengths propagate at different effective group velocity angles as shown in Fig. 1, thus demultiplexing different wavelengths by spatial beam shifting. We have previously discussed that nonperiodic thin-film stacks offer superior wavelength splitting characteristics due to the larger design freedom [6]. Here, we present experimental results demonstrating a four-channel wavelength demultiplexer. Furthermore, we discuss the maximum number of channels theoretically possible for the given design.

We designed and experimentally tested a 66-layer nonperiodic thin-film stack consisting of alternating layers of  $\text{SiO}_2$  ( $n = 1.46$  at 830 nm) and  $\text{Ta}_2\text{O}_5$  ( $n = 2.06$ ) with a total stack thickness of 13.4  $\mu\text{m}$  for operation at an incidence angle  $\theta_{\text{in}}$  of  $54^\circ$  [6]. We choose to operate the stack in reflection as shown in Fig. 1. To prevent reflections off the front of the stack, we used a “tapered” Bragg stack as the starting design [7]. In such a Bragg stack, the periodicity is slowly “turned on” by increasing the amount of high index material in each period. This is equivalent to tapering a surface corrugated structure [1]. Next, we employed numerical refinement techniques [8]

Manuscript received February 21, 2003; revised May 5, 2003. This work was supported by the Defense Advanced Research Projects Agency (DARPA) Optocenters Program. The work of M. Gerken was supported by the Sequoia Capital Stanford Graduate Fellowship.

The authors are with the Edward L. Ginzton Laboratory, Stanford University, Stanford, CA 94305 USA (e-mail: gerken@stanford.edu).

Digital Object Identifier 10.1109/LPT.2003.815318

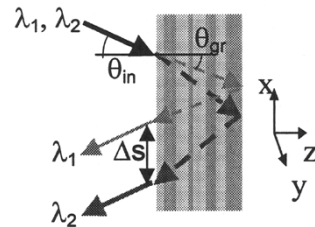


Fig. 1. Spatial wavelength demultiplexer.

on the tapered Bragg stack to achieve a design with a linear shift upon reflection as a function of wavelength. A detailed discussion of the physics and design of this structure is given in [6]. Since we operate the dielectric stack at an angle, the device is polarization sensitive. This particular design only works for p-polarization.

The designed stack exhibits an 18- $\mu\text{m}$  linear shift  $\Delta s$  along the exit interface between 822 and 842 nm for a single reflection [6]. The effective group propagation angle  $\theta_{\text{gr}}$  changes from  $17^\circ$  to  $46^\circ$  corresponding to a dispersion of  $1.5^\circ/\text{nm}$ . Depending on the application, nonperiodic stacks with very different dispersion values can be designed [6], such that the dispersion of a stack is not on its own a good figure of merit to judge the performance of the device. More significant is the total shift, since the number of separable channels  $N_{\text{channels}}$  is given by the spatial shift  $\Delta s$  divided by the spatial extent per channel  $\Delta x$ . The spatial shift can be increased by performing multiple reflections off the stack [2]. The resulting number of channels  $N_{\text{channels}}$  is given by (1), where  $N_b$  is the number of bounces off the stack:

$$N_{\text{channels}} = 1 + \frac{N_b \Delta s}{\Delta x} = 1 + \frac{N_b \Delta s \cos(\theta_{\text{in}})}{c_{\text{crosstalk}} w_0}. \quad (1)$$

The largest number of channels is obtained if all wavelengths are focussed at the same position. This condition is fulfilled for a linear shift with wavelength. The Gaussian spot size along the exit interface is then  $w_0 / \cos(\theta_{\text{in}})$  for all channels. The crosstalk is largest between adjacent channels. Defining  $c_{\text{crosstalk}}$  as the ratio of  $\Delta x$  to the spot size along the interface, we obtain that channels separated by twice the projected Gaussian spot size, i.e.,  $c_{\text{crosstalk}} = 2$ , have an adjacent channel crosstalk of approximately  $-15$  dB. For a crosstalk of less than  $-30$  dB,  $c_{\text{crosstalk}}$  should be chosen as 3.2, and for  $-40$  dB as 3.8. In the following we consider the case of  $c_{\text{crosstalk}} = 2$ .

Fig. 2 shows a scaled schematic of our device. The multiplexed Gaussian beam is incident at an angle onto the thin-film stack from the substrate side ( $n_s = 1.52$ ). The spatial separation is increased by performing eight bounces off the stack.

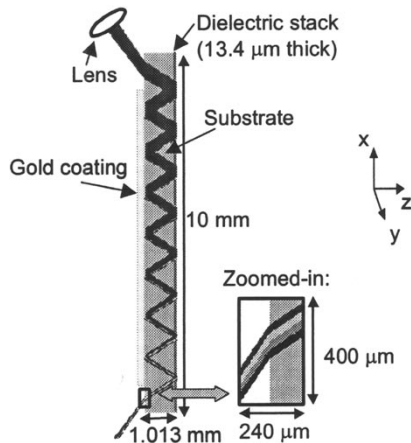


Fig. 2. Scaled device schematic. Different wavelengths incur a different spatial shift upon reflection off the dielectric stack and are spatially separated.

A lens focuses the light at the exit side to minimize the spatial extent per channel at the output. The wavelength splitting occurs solely within the multilayer stack. Beams of different wavelength propagate in parallel everywhere else. The total device size of 10 mm in the  $x$  direction is mainly determined by the substrate thickness of 1 mm. The substrate is needed to spatially separate different bounces, which prevents mixing of light from the penultimate and the ultimate bounces at the exit. Thus, the minimum substrate size  $L_s$  is given by (2), where  $\theta_s$  is the propagation angle in the substrate:

$$L_s > \frac{N_b \Delta s}{2 \tan(\theta_s)}. \quad (2)$$

Reducing the substrate thickness to 100  $\mu\text{m}$  would shrink the overall dimensions of the demultiplexer by a factor of 10 without changing the performance characteristics (mechanical stability permitting). In the  $y$  direction the device only needs to be as wide as the incident beam.

We tested the design by focusing the p-polarized light of a tunable continuous wave Ti-Sapphire laser at a  $54^\circ$  incidence angle onto the structure. As we are operating close to the Brewster angle for the quartz substrate, no antireflection coating is needed. The 9.2- $\mu\text{m}$  spot size corresponds to a 15.7- $\mu\text{m}$  spot size projected along the  $x$  direction. We used a lens to project a magnified image of the exit interface onto a CCD camera. As the beam propagates through a plate at an angle, astigmatism is introduced, and the focal points for the  $x$ - and the  $y$  direction are not identical anymore leading to elongated beam shapes. To obtain a simultaneous focus in both directions a cylindrical lens would be needed. Fig. 3 shows the experimentally observed shift along the  $x$  direction for the 66-layer nonperiodic stack. Experiment and theory are performed for one bounce off the stack and results are multiplied by eight. The shifts for the four wavelength channels discussed in Fig. 4, as experimentally obtained after eight bounces through the structure, are given by the circles. We see that eight bounces result exactly in an eight-fold shift. Also shown is the shift as a function of wavelength for a 200-layer periodic stack at  $45^\circ$  incidence angle and p-polarization [6]. The experimental results for one bounce are scaled to a center wavelength of 830 nm and multiplied by eight for

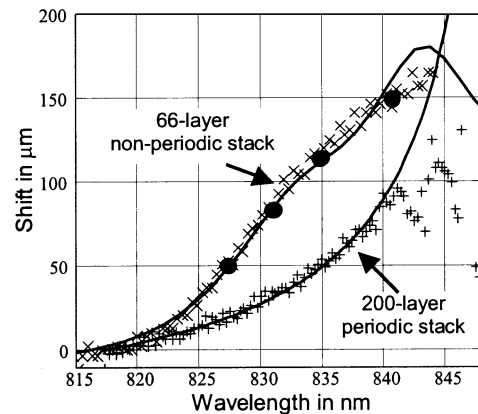


Fig. 3. Shift along the  $x$  direction after one bounce multiplied by eight as observed in experiment for a 66-layer non-periodic stack ( $\times$ ) and a 200-layer periodic stack ( $+$ ) and calculated theoretically (lines). The circles indicate the shift measured after eight bounces through the structure at the wavelengths of the four channels in Fig. 4.

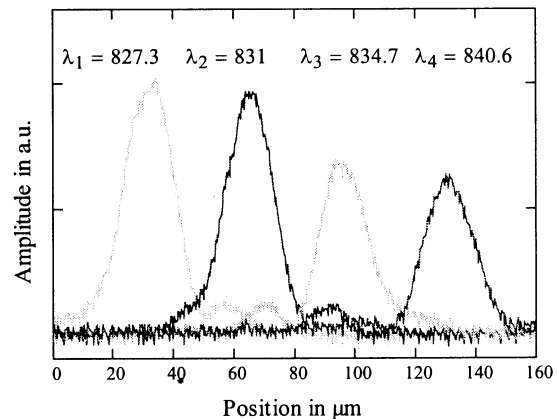


Fig. 4. Four overlapped CCD traces along the  $x$  direction. Using eight bounces through a single 66-layer dielectric stack at a  $54^\circ$  incidence angle we can separate four beams by their Gaussian beam widths. The channel wavelengths given in the plot are in units of nm.

easier comparison. Beams of finite width are composed of a finite range of input angles, and different input angles correspond to different dispersion curves. Thus, the high theoretical shift (calculated assuming plane waves) of the periodic stack closer to the bandedge at 855 nm is not achievable for finite width beams. The finite beam width is also responsible for the lower than expected shift above 840 nm for the nonperiodic stack. The superior dispersion characteristics of the nonperiodic stack in terms of linearity and total shift are clearly visible. In addition the nonperiodic stack has just a third of the layers.

Fig. 4 demonstrates that the shift of the nonperiodic stack is sufficient to separate four beams by their Gaussian beam widths [9]. The first three beams have a channel spacing of 3.7 nm. The wavelength spacing between the third and fourth channels is 5.9 nm, being chosen larger because of the reduced dispersion. The amplitudes of the beams are decreasing with wavelength, since the dielectric stack has a lower reflectance for longer wavelengths leading to transmission loss through the stack. Furthermore, the experimental efficiency was low at all wavelengths due to a chromium layer under the gold coating. Simulations predict a maximum loss of 35% after eight bounces

with pure gold coatings applied on both sides of the stack. Using dielectric reflection coatings reduces this loss further. The slight beam distortions visible in Fig. 4 are caused by clipping in the imaging optics and would not be present in the actual device.

To increase the number of channels or to reduce the crosstalk between the four channels, the beams could be focussed to a smaller spot size or more bounces could be performed off the stack. The number of bounces is ultimately limited, though, by the widening of the Gaussian beam. To prevent an overlap at the input of the incoming beam with beam size  $w_{\text{in}}$  and the first reflection off the stack, condition (3) has to remain valid.

$$2w_{\text{in}}(\lambda, w_0, L_s, \theta_s, N_b) \leq 2L_s \sin(\theta_s). \quad (3)$$

Calculating  $w_{\text{in}}$  using the formula for Gaussian beam propagation [10], we find that the maximum number of bounces  $N_b$  is related to the spot size of the beam in vacuum  $w_0$  as given in (4) for propagation distances much larger than the Rayleigh range.

$$N_b \leq \frac{\pi w_0 \sin(\theta_{\text{in}}) (1 - \sin(\theta_{\text{in}})^2 / n_s^2)}{2\lambda \cos(\theta_{\text{in}})}. \quad (4)$$

Employing refocussing more bounces could be performed, but additional lenses are needed. Substituting (4) into (1), we obtain the maximum number of channels as given in (5).

$$N_{\text{channels}} \leq 1 + \frac{\Delta s \pi \sin(\theta_{\text{in}}) (1 - \sin(\theta_{\text{in}})^2 / n_s^2)}{\lambda 2c_{\text{crosstalk}}}. \quad (5)$$

Interestingly, the maximum number of channels for the device configuration given in Fig. 2 does not depend on the spot size or the number of bounces as long as the maximum number of bounces is performed as calculated by (4). For the 66-layer design discussed here, (5) predicts a maximum of seven channels for  $c_{\text{crosstalk}} = 2$ . In order to obtain this maximum number, either the number of bounces has to be increased to 17 or the spot size has to be reduced to 4.5  $\mu\text{m}$ . To obtain more than seven channels, a stack with a larger total shift has to be designed, demonstrating again that the total shift  $\Delta s$  is a better figure of merit than the dispersion. We chose to operate the design around 830 nm because of the available tunable laser, but it can easily be scaled to the 1300- or 1550-nm wavelength regime. Upon scaling all layers by the same factor, the spatial shift and the channel spacing are scaled as well. Therefore, the 100- $\mu\text{m}$  shift and 4-nm channel spacing at 830 nm correspond to a 187- $\mu\text{m}$  shift and 7.5-nm channel spacing at 1550 nm. Scaling the spot

size by the same factor, the same number of channels is obtained as seen from (4) and (5).

Here, we have shown that a thin-film stack can be designed to exhibit a rapid change in the effective group propagation angle with wavelength. We demonstrated a nearly linear 100- $\mu\text{m}$  shift over a 13-nm wavelength range. This device principle is not limited to this type of shift and wavelength range. Thin-film filter design techniques can be used to design a wide range of dispersion characteristics with wavelength. The stack could, for example, be designed to exhibit dispersion over a much narrower or broader wavelength range, or the dispersion could be designed to be linear with frequency instead of wavelength or even staircase-like [11]. In conclusion, group velocity effects in thin-film filters can be utilized to obtain compact, cost-effective wavelength multiplexing and demultiplexing devices that use a single multilayer structure to separate multiple beams.

#### ACKNOWLEDGMENT

The authors are pleased to acknowledge A. Clark of JDS Uniphase for the growth of the sample.

#### REFERENCES

- [1] R. Zengerle, "Light propagation in singly and doubly periodic planar waveguides," *J. Mod. Opt.*, vol. 34, no. 12, pp. 1589–1617, 1987.
- [2] B. E. Nelson, M. Gerken, D. A. B. Miller, R. Piestun, C.-C. Lin, and J. S. Harris Jr., "Use of a dielectric stack as a one-dimensional photonic crystal for wavelength demultiplexing by beam shifting," *Opt. Lett.*, vol. 25, no. 20, pp. 1502–1504, 2000.
- [3] T. Baba and M. Nakamura, "Photonic crystal light deflection devices using the superprism effect," *IEEE J. Quantum Electron.*, vol. 38, pp. 909–914, July 2002.
- [4] L. Wu, M. Mazilu, T. Karle, and T. F. Krauss, "Superprism phenomena in planar photonic crystals," *IEEE J. Quantum Electron.*, vol. 38, pp. 915–918, July 2002.
- [5] H. Kosaka, T. Kawashima, A. Tomita, M. Notomi, T. Tamamura, T. Sato, and S. Kawakami, "Superprism phenomena in photonic crystals," *Phys. Rev. B*, vol. 58, no. 16, pp. R10 096–R10 099, 1998.
- [6] M. Gerken and D. A. B. Miller, "Multilayer thin-film structures with high spatial dispersion," *Appl. Opt.*, vol. 42, no. 7, pp. 1330–1345, 2003.
- [7] N. Matuschek, F. X. Kärtner, and U. Keller, "Theory of double-chirped mirrors," *IEEE J. Select. Topics Quantum Electron.*, vol. 4, no. Mar./Apr., pp. 197–208, 1998.
- [8] J. A. Dobrowolski and R. A. Kemp, "Refinement of optical multilayer systems with different optimization procedures," *Appl. Opt.*, vol. 29, no. 19, pp. 2876–2893, 1990. and references herein.
- [9] M. Gerken and D. A. B. Miller, "Thin-film (DE)MUX based on group-velocity effects," presented at the ECOC 2002, Copenhagen, Denmark, Sept. 8–12, 2002. Paper 11.3.3.
- [10] A. E. Siegman, *Lasers*. New York: Univ. Sci. Books, 1986.
- [11] M. Gerken and D. A. B. Miller, "Thin-film (DE)MUX based on step-like spatial beam shifting," presented at the IEEE Lasers and Electro-Optics Society 2002 Annual Meeting, Glasgow, Scotland, Nov. 10–14, 2002. Paper ThV 3.